Electronic Supplementary Material (ESI) for Nanoscale.

Supporting Information

Ultrathin MOF nanosheets and its Mixed-Matrix Membranes for ammonia and aliphatic amine sensing in water

Ritu Ladhi [a], Arshminder Kaur Dhillon, [a], Monika Singh[a]*

[a] Institute of Nano Science and Technology, Knowledge City, Sector-81, Mohali-140306, Punjab, INDIA

*Corresponding author: monika@inst.ac.in

Contents

Section S1: General information

Physical Measurements FT-IR spectra were recorded on a PerkinElmer Spectrum I spectrometer with samples prepared as KBr pellets in the range of 4000-400 cm^{-1}. The solid state (DRS) and solution state UV-*Vis* spectra of compound and analyte were explored by UV/Vis spectrophotometer (Shimadzu UV-2600). The morphological studies were carried out by field emission scanning electron microscopy (FESEM) on a JEOL JSM-7600F system. TGA analysis was carried out using Perkin–Elmer Pyris 1 model on well ground samples in flowing nitrogen atmosphere at a heating rate of 10 °C/min. Emission spectra were recorded using an EDINBURGH instrument FS5 spectrophotometer. Time-resolved lifetime decay profiles were measured using photoluminescence Fluorolog 3-221 (Horiba Scientific) single photon counting controller. Powder X-ray diffraction analysis was carried out on a Bruker D8-Advance Eco Diffractometer using Ni-filtered Cu Kα radiation at room temperature. The data were collected over the range of $5° < 2\theta < 60°$ with a step size of 0.01°. The BET nitrogen isotherm analysis was carried out on Quantachrome ASiQwin at 300 K.

Theoretical calculations Geometry optimization and frequency calculations are performed using Becke's three parameter functional in combination with the Lee-Yang-Parr correlation functional (B3LYP) and 6-31G basis set. Gaussian 09 suite of programs is used for all the calculations.

Experimental Procedures

Materials

Nickel (II) nitrate hexahydrate ($Ni(NO_3)_2.6H_2O$, ≥98.0%), sodium borohydride ($NaBH_4$, ≥99%), 1,3,5tricarboxylic acid (H_3BTC, 95%), N,N-dimethylformamide (DMF, ≥99.8%), Ethanol and Methanol. All chemicals were purchased from Sigma Aldrich. All the chemicals were used as obtained without further purification. The water used was deionized water.

Synthesis of nickel-oxide nanosheets (NiO-NS)

For synthesis of NiO NS, two different solutions were prepared: Solution A consisted of 0.582 g of $Ni(NO_3)_2 \cdot 6H_2O$ in 50.0 mL of water, while Solution B contained of 0.2 g of $NaBH_4$ dissolved in 20 mL of water. Solution A was stirred continuously for 10 minutes to ensure complete dissolution of the chemicals, then Solution B was added drop by drop to

Solution A. After allowing the reaction to proceed for 5 minutes, the resulting product was subjected to centrifugation and washed with ethanol three times. Finally, it was dried under vacuum at room temperature for two days.

Synthesis of Ni-*btc* nanosheets

A mixture of NiO-NS (58.8 mg) and H_3btc (24.1 mg) was immersed in 10.0 ml of EtOH/DMF/H_2O (1:1:1) solution with continuous stirring for 10 mins. After that, mixed solution was encapsulated in 25mL Teflon-line stainless steel autoclave and was left in oven at 100 ℃ for 24 hrs. The product was obtained by centrifugation, washed twice by DMF, immersed in methanol overnight and finally dried under vacuum at 40 ℃.

Model wastewater preparation: An aqueous solution was prepared using 1 L of distilled water, 80 mg of $CaCl_2$, 30 mg of $Mg(NO_3)_2$, 20 mg of K_2SO_4, 60 mg of Na_2SO_4 and used for preparation of the suspension.

Section S2: Characterization of Ni-*btc* NS MOF

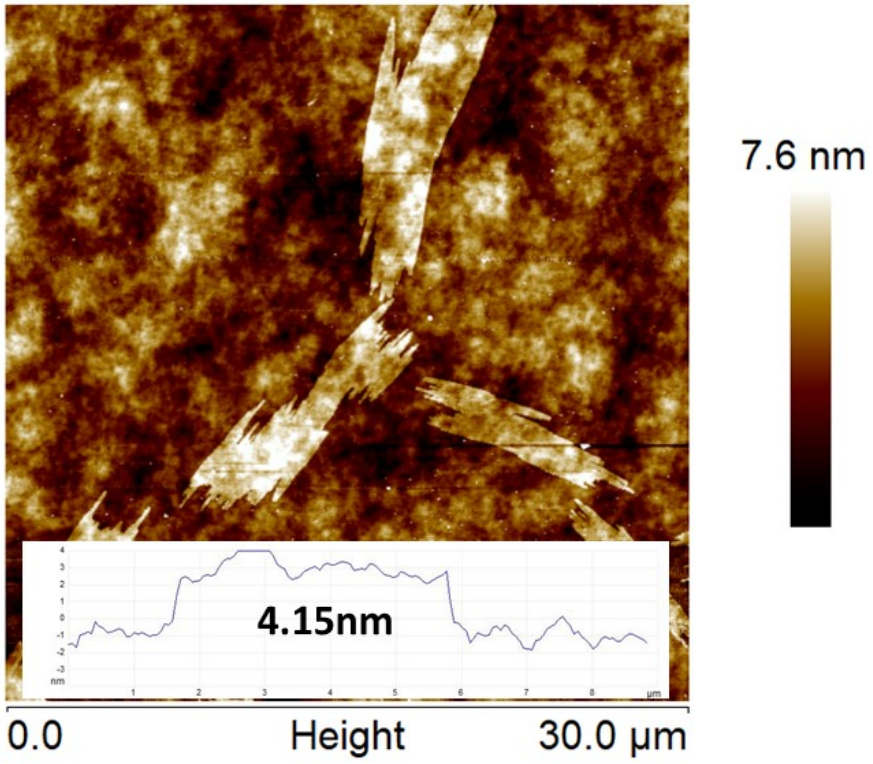

Figure S1. AFM image of **Ni-*btc*** ultrathin nanosheets with thickness of 4.15 nm

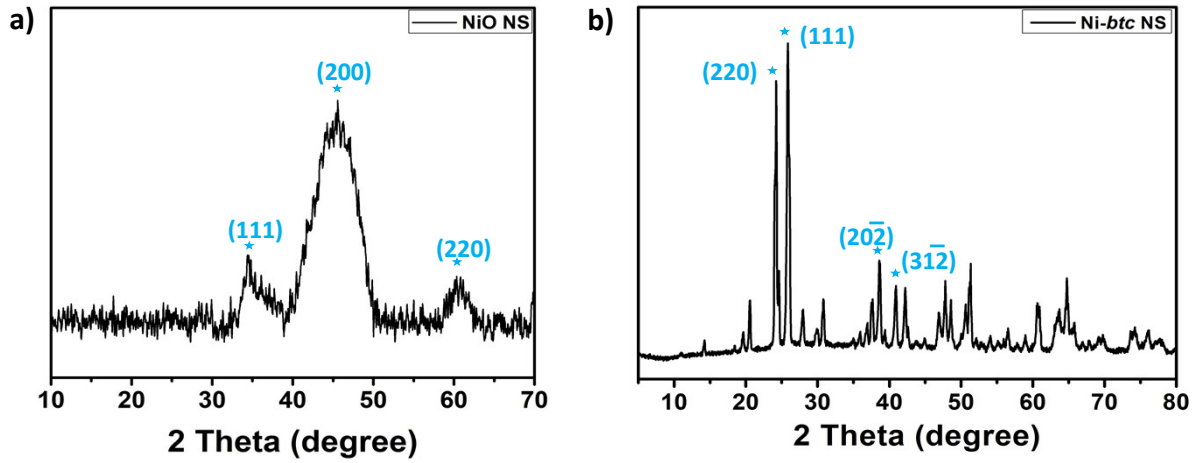

Figure S2. PXRD profiles of a) **NiO NS** (JCPDS card no. #47-1049) b) **Ni-*btc* NS**

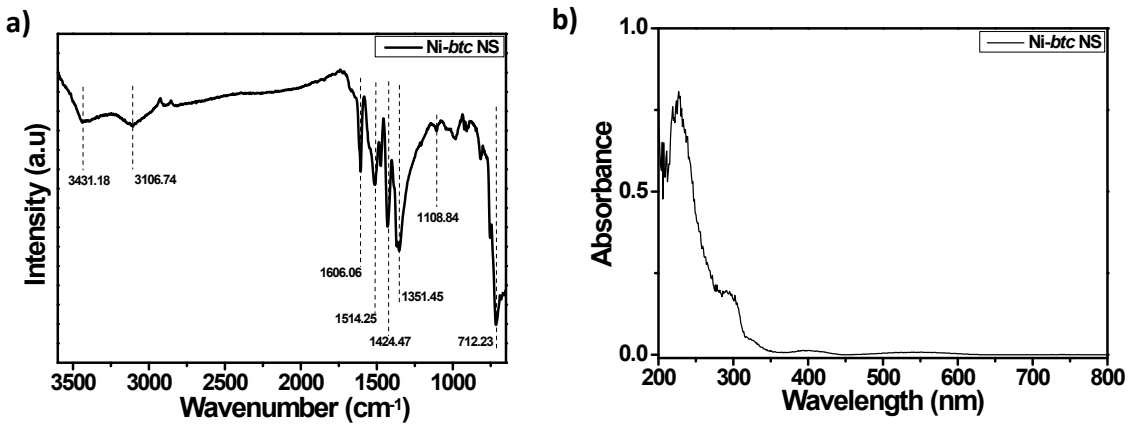

Figure S3. a) FT-IR and b) Solid-state UV-*Vis* spectrum of **Ni-*btc* NS**

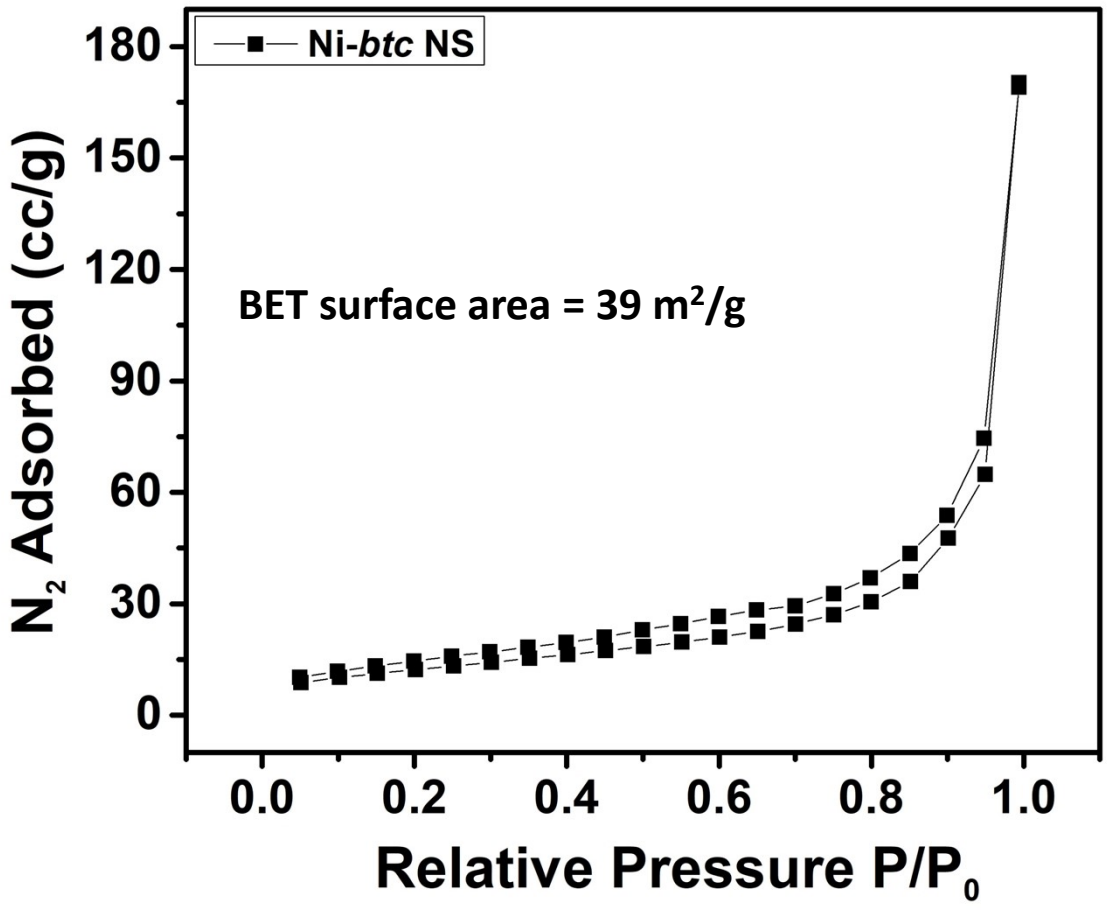

Figure S4. N_2 adsorption Isotherm of **Ni-*btc* NS**

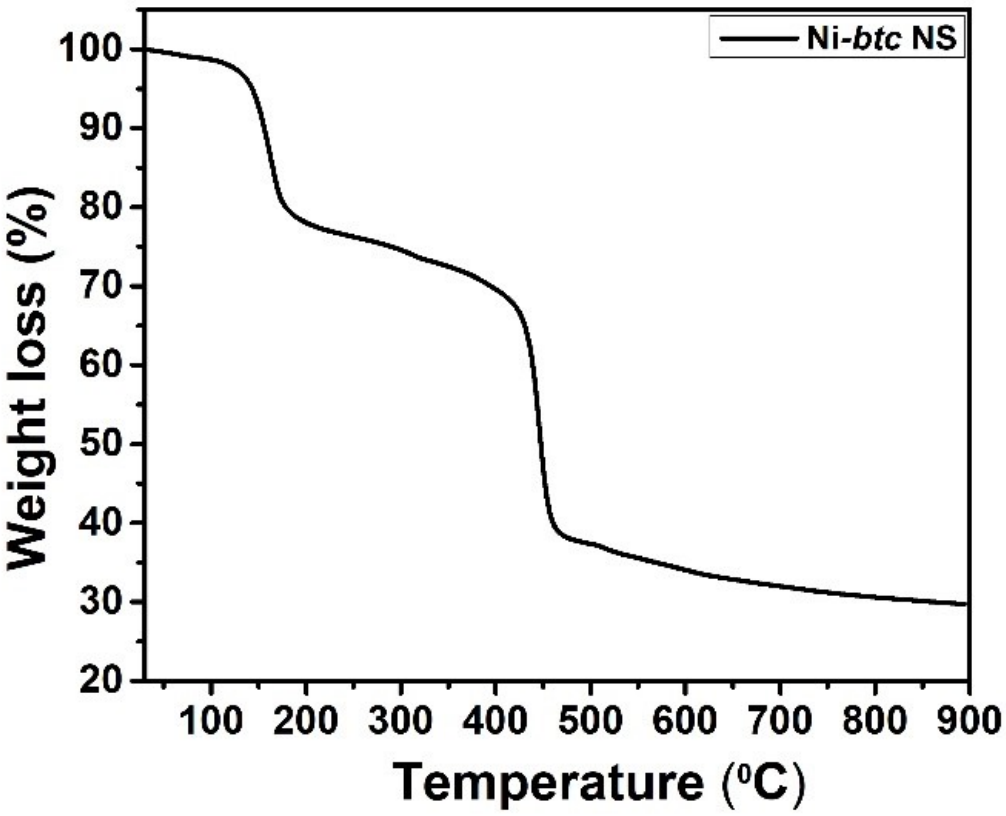

Figure S5. TGA spectra **Ni-*btc* NS**

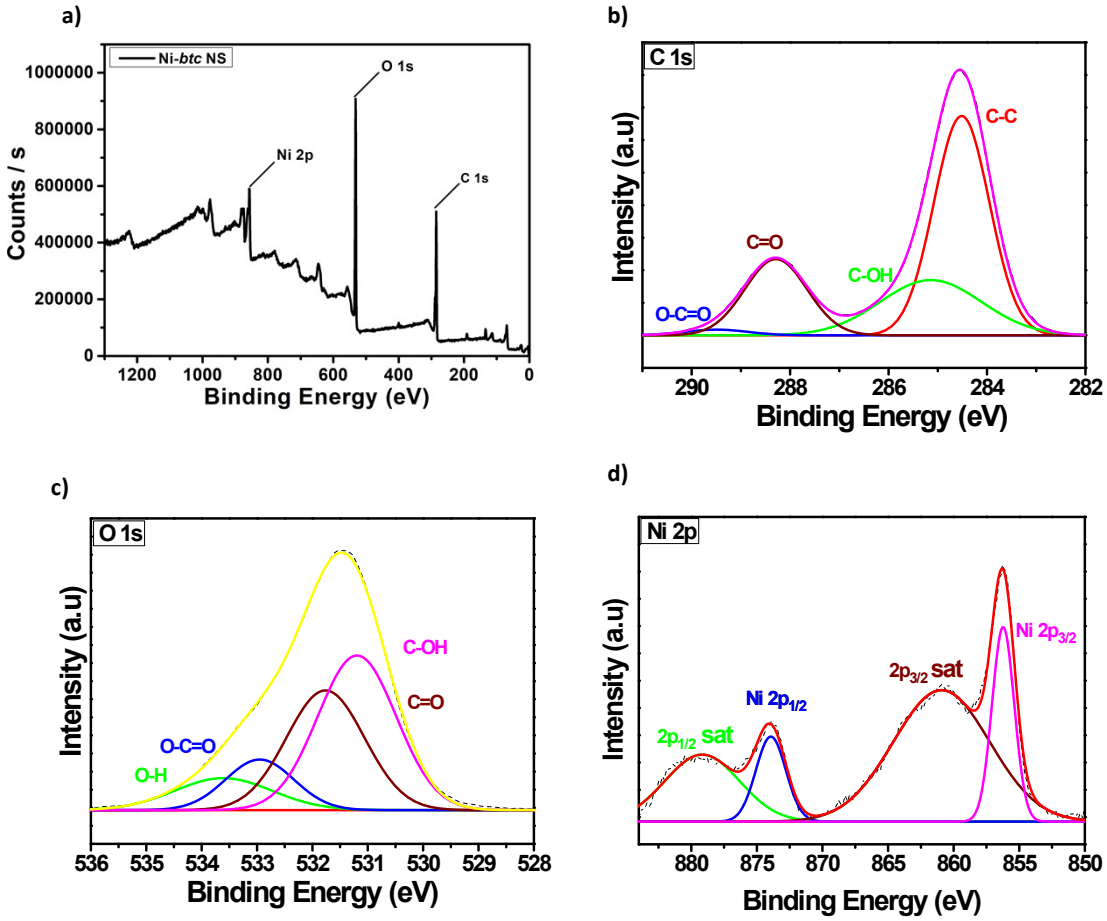

Figure S6. a) XPS Survey spectra, and **b)** Curve-resolved XPS of C1s**, c)** O1s and **d)** Ni 2p of **Ni-*btc* NS**

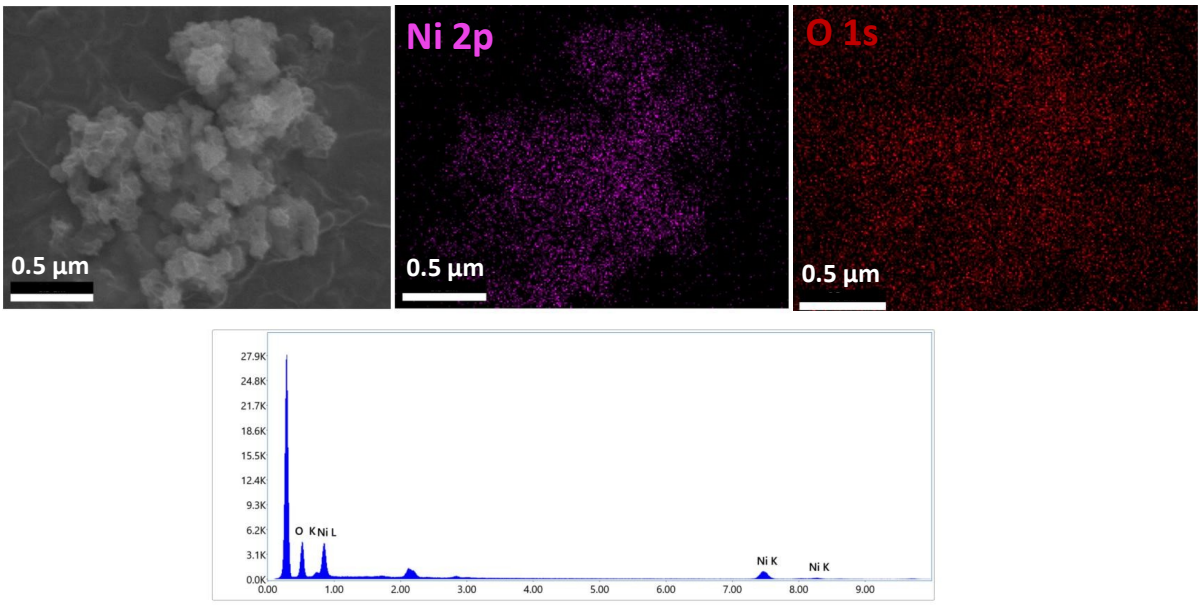

Figure S7. EDS mapping image of **NiO NS**

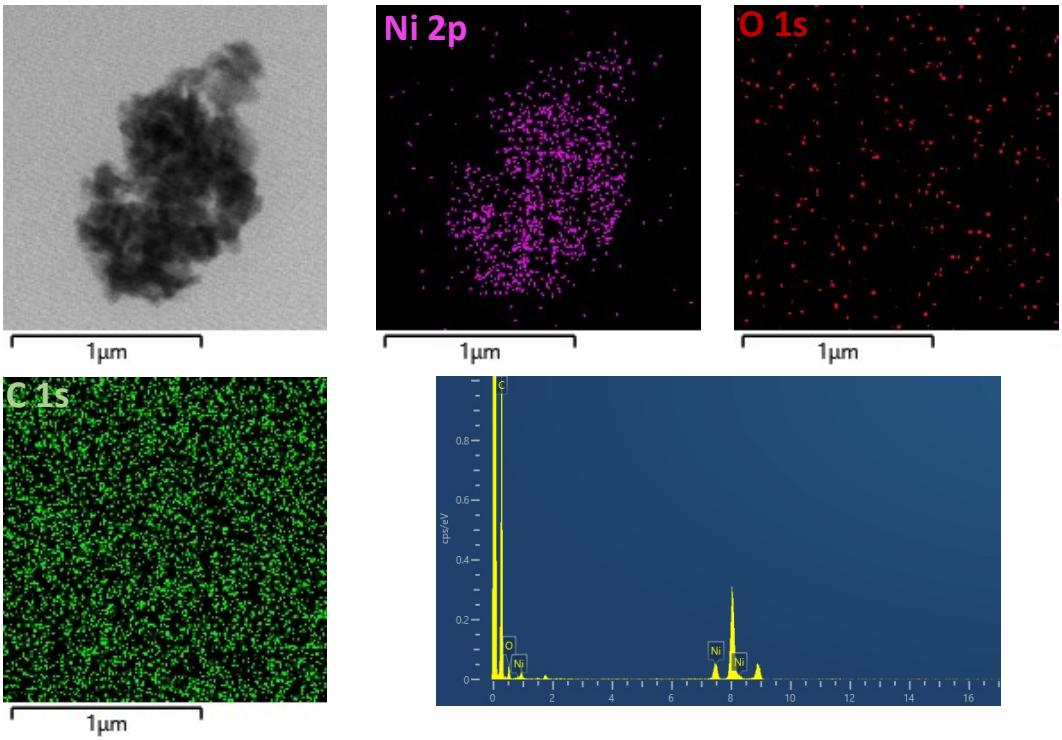

Figure S8. EDS mapping image of **Ni-*btc* NS**

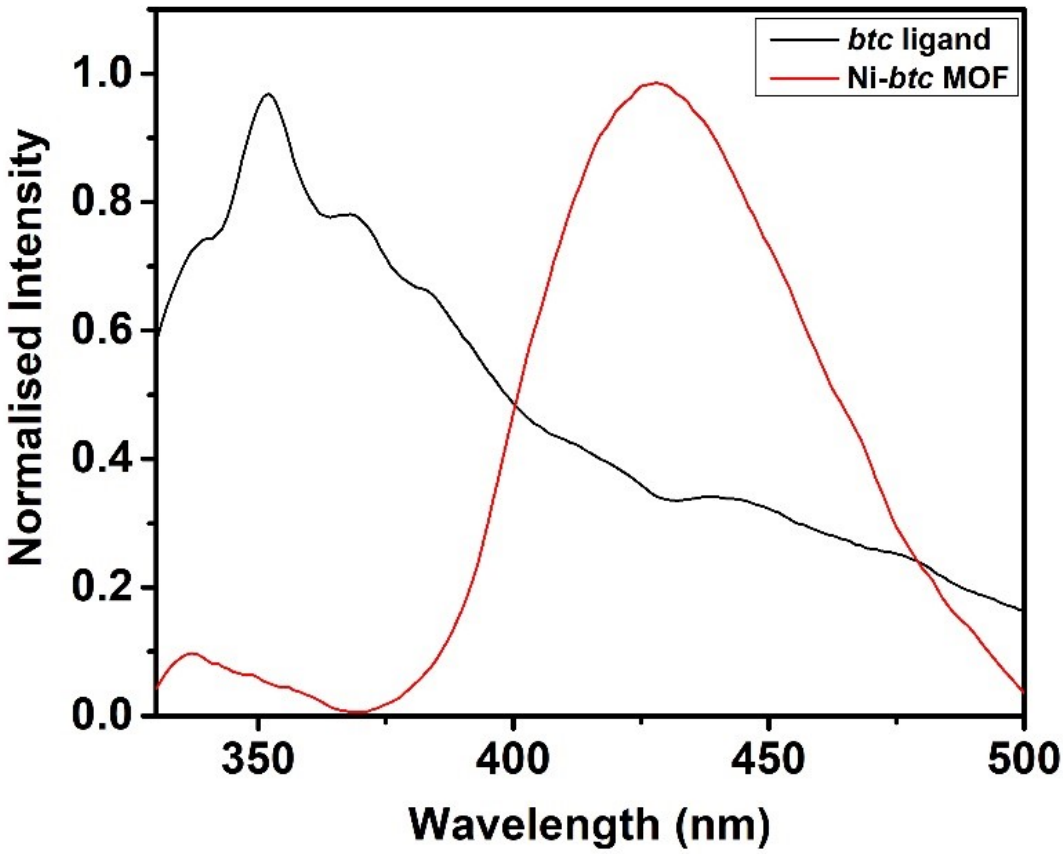

Figure S9. Emission spectra of **Ni-*btc*** and ***btc*** ligand.

Section S3: Titration curves, Detection limit calculation and lifetime measurements

Detection limit was calculated using the following equation:

Detection limit = 3σ/m

Where 'σ' is the calculated standard deviation from five blank measurements and 'm' is the slope obtained from the plot of fluorescence emission with increasing concentration of analytes.

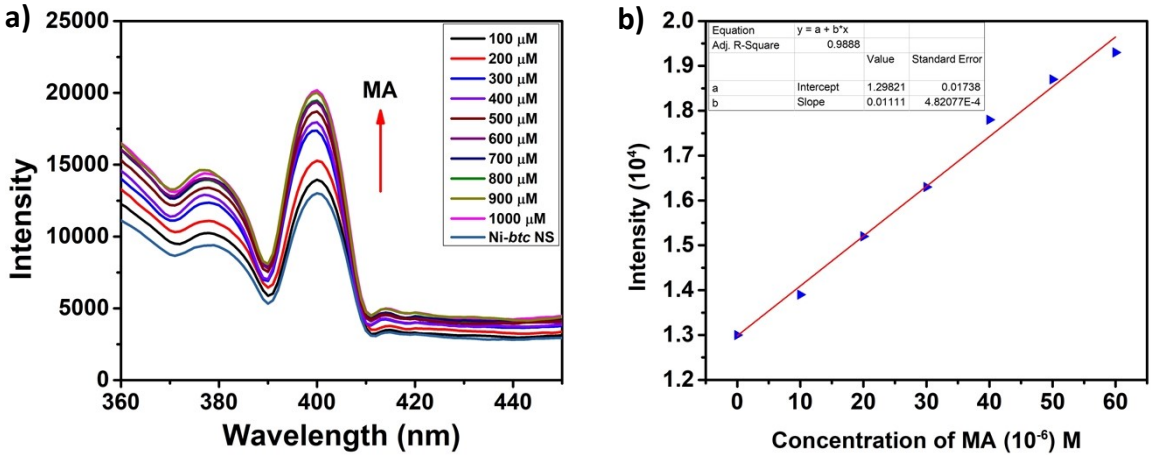

Figure S10. a) Change in emission spectrum of **Ni-*btc* NS** dispersed in water upon addition of Methyl Amine (MA) b) Determination of detection limit through fitting of the linear region of fluorescence intensity of **Ni-*btc* NS** upon adding different concentration of MA to it at λ_{emi} = 400 nm (upon λ_{exc} = 310 nm).

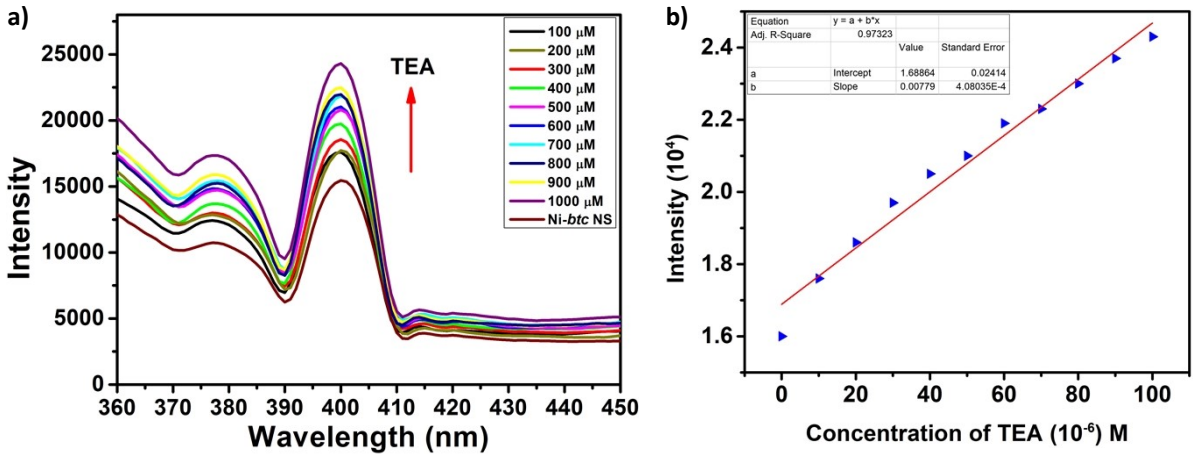

Figure S11. a) Change in emission spectrum of **Ni-*btc* NS** dispersed in water upon addition of Triethyl Amine (TEA) b) Determination of detection limit through fitting of the linear region of fluorescence intensity of **Ni-*btc* NS** upon adding different concentration of TEA to it at λ_{emi} = 400 nm (upon λ_{exc} = 310 nm).

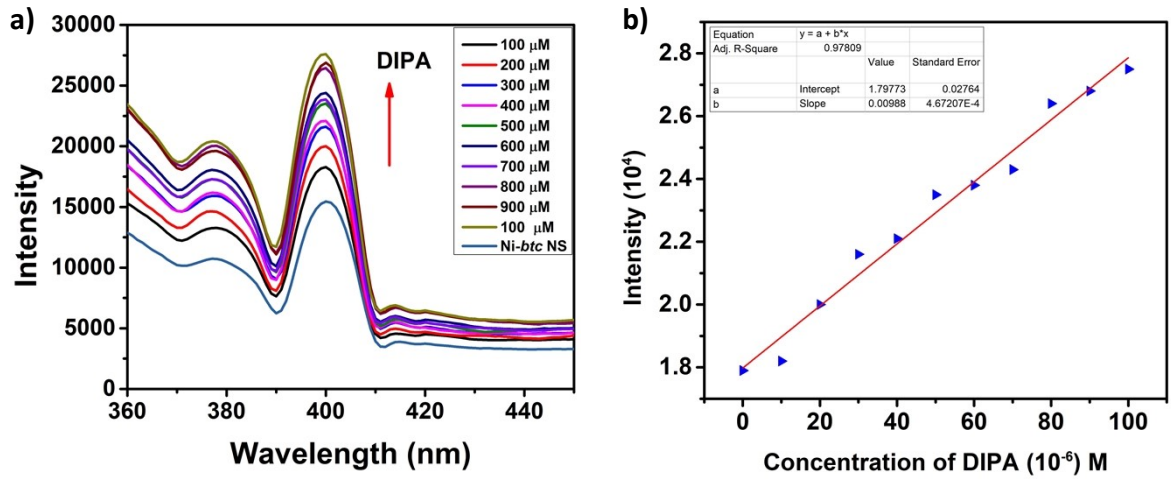

Figure S12. a) Change in emission spectrum of **Ni-*btc* NS** dispersed in water upon addition of Diisopropyl Amine (DIPA) b) Determination of detection limit through fitting of the linear region of fluorescence intensity of **Ni-*btc* NS** upon adding different concentration of DIPA to it at λ_{emi} = 400 nm (upon λ_{exc} = 310 nm).

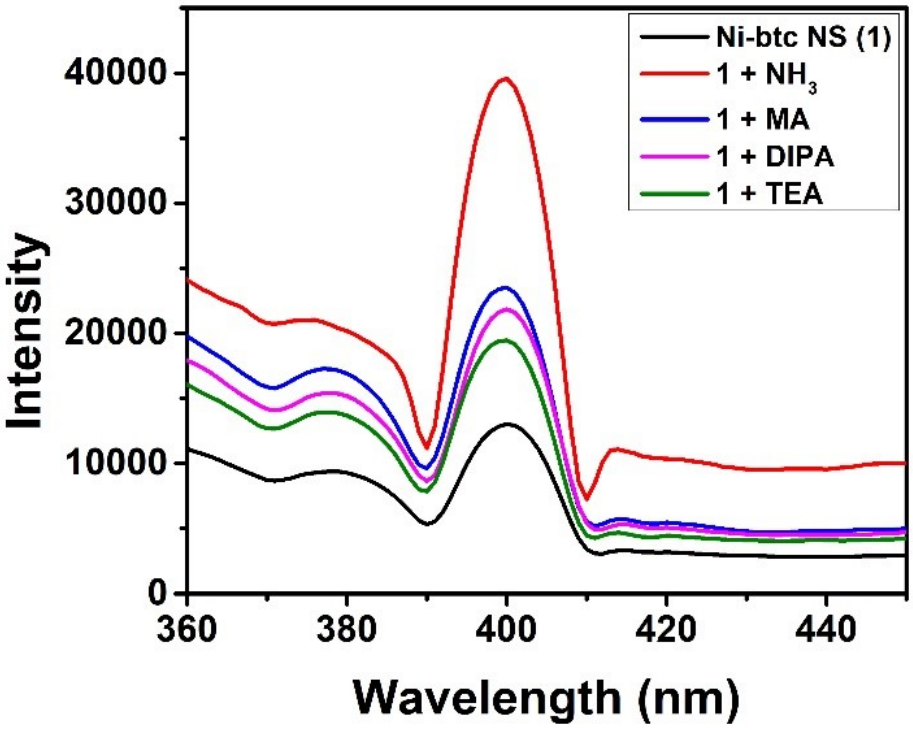

Figure S13. Comparison of fluorescence enhancement of **Ni-*btc* NS** (1) with different amines (0.5 mM)

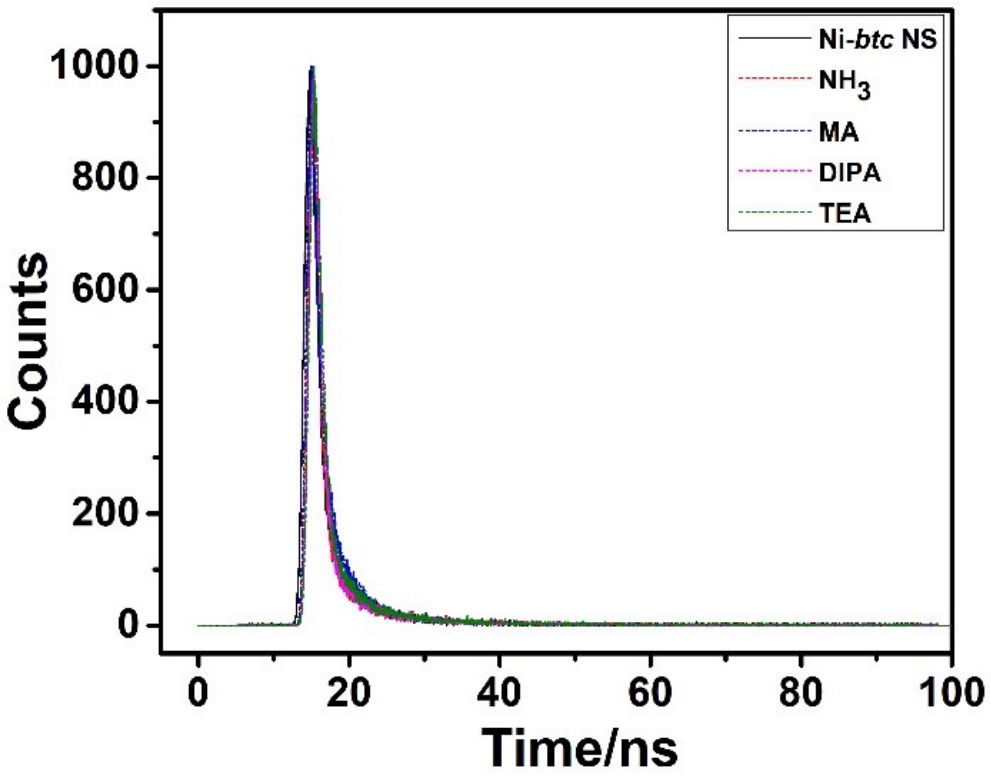

Figure S14. Lifetime decay profiles of **Ni-*btc* NS** before and after immersing in NH_3, MA, DIPA and TEA

Table S1. Average lifetime of **Ni-*btc* NS** before and after addition of amines

	Ni-*btc* NS (1)	**1+ NH_3**	**1+ MA**	**1+ DIPA**	**1+ TEA**
τ_1 (ns)	1.01	0.72	0.72	0.81	0.91
α_1	0.76	0.75	0.73	0.77	0.74
τ_2 (ns)	6.53	5.98	5.96	6.99	6.49
α_2	0.24	0.25	0.27	0.23	0.26
$<\tau>$ (ns)	4.77	4.57	4.67	5.25	4.89

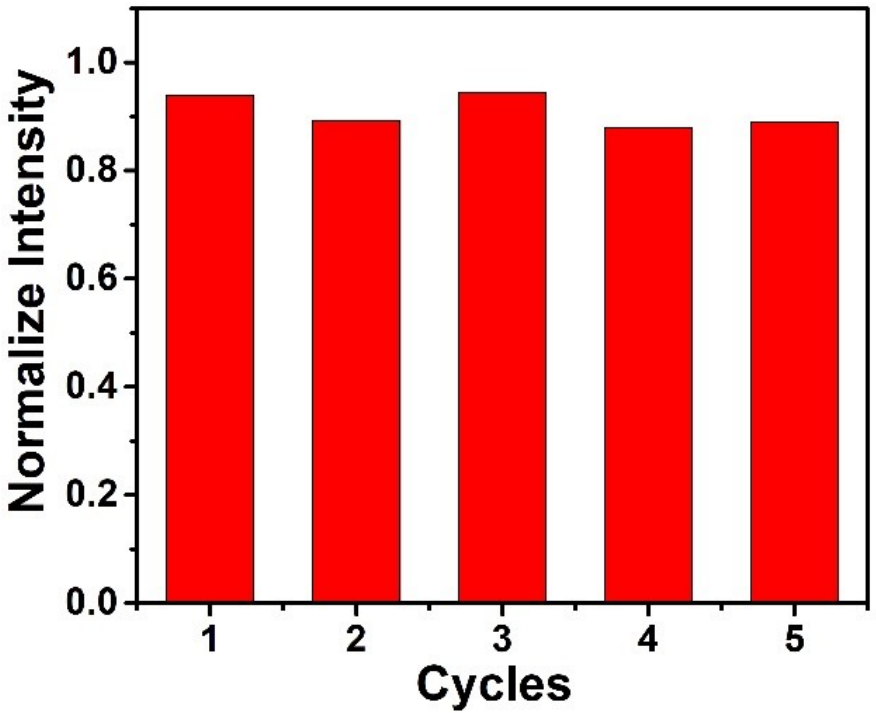

Figure S15. Five consecutive detection-regeneration cycles of **Ni-*btc* NS** for NH_3 sensing

Section S4: HOMO LUMO energy calculations

Electrochemical measurements

To obtain HOMO and LUMO values for the MOF, cyclic voltammetry plots were collected for **Ni-*btc* NS MOF**. CV was recorded with the help of three electrode cell setup using Fluorine-doped Tin Oxide (FTO) as the working electrode, platinum as the counter electrode, and Ag/AgCl as a reference electrode. 0.1M tetrabutylammonium hexafluorophosphate in acetonitrile was used as an electrolyte with a scan rate of 100 mV/s. The onset oxidation potential and reduction potential values obtained from CV measurements were used to calculate the HOMO and LUMO energy levels with the help of the following equation:

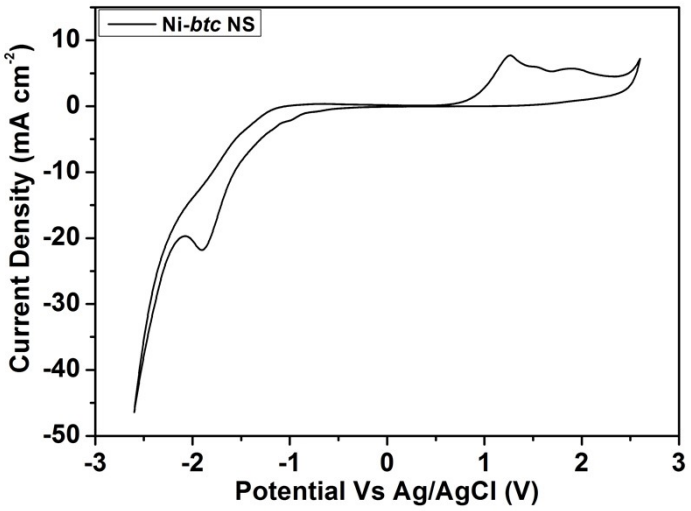

Figure S16. Cyclic Voltammetry plot of **Ni-*btc* NS** obtained in acetonitrile medium with scan rate of 100 mV/s.

E_{HOMO} = -e [E_{ox} onset + 4.741] eV and **E_{LUMO} = -e [E_{red} onset + 4.741] eV.**

Similarly, the band gap was calculated using the following formula: **$E_g = E_{LUMO} - E_{HOMO}$,** and the band gap resulted as 2.19 eV for both the frameworks.

Computational Methods

HOMO and LUMO energies and Dipole moment calculated for amines using Gaussian 09 package and their subsequent geometry optimization was carried out at B3LYP level of DFT.[1]

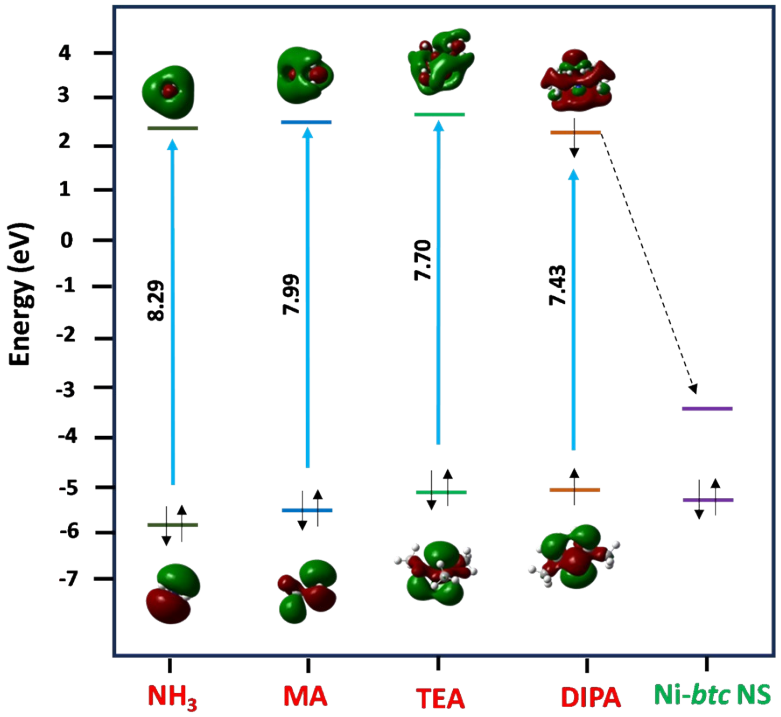

Figure S17. HOMO and LUMO energy levels of amines analytes.

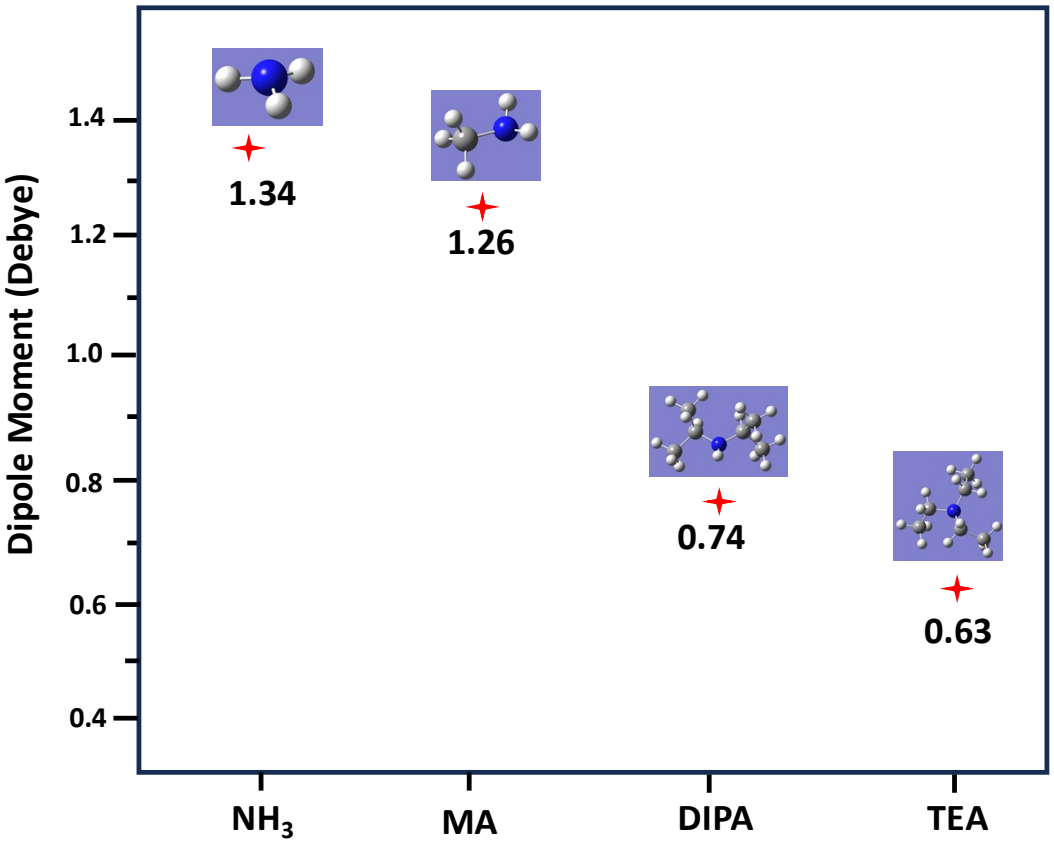

Figure S18. Dipole moment of amines analytes.

Table S2. HOMO and LUMO energies calculated for amines

	E_{HOMO} (eV)	E_{LUMO} (eV)
NH_3	-5.98	2.32
MA	-5.60	2.39
TEA	-5.24	2.45
DIPA	-5.22	2.21

Table S3. Comparative list of various fluorescent CPs / MOFs including **Ni-*btc* NS** that have been used for sensing of ammonia in water solvent.

Serial No.	**Metal Organic Framework**	**Analyte**	**Luminescence type**	**LOD**	**Reference**
1	**Ni-*btc* NS**	Ammonia	Turn ON	0.00075 ppm	**This work**
2	UiO-68(bod)	Ammonia	Turn ON	0.0065 ppm	2
3	SNNU-88	Ammonia	Turn OFF	~1.5 ppm	3
4	$\{Cd_4(HIDCPy)_6].4DMF.4C_2H_8N.H_2O\}_n$	Ammonia	Turn ON	NA	4

Abbreviation: H_3btc = benzene tricarboxylic acid; **bod** = 2,1,3-benzoxadiazole; **SNNU-88** = magnesium–organic framework; **H_2IDCPy** = 2-(pyridine-2-yl)-1H-imidazole-4,5-dicarboxylic acid

Table S4. Comparative list of various fluorescent CPs / MOFs including Ni-*btc* NS that have been used for sensing of various amines in water solvent.

Serial No.	**Metal Organic Framework**	**Analyte**	**Luminescence type**	**LOD**	**Reference**
1	Ni-*btc* NS	MA DIPA TEA	Turn ON	0.297 µM 0.330 µM 0.424 µM	This work
2	$[\{Zn(L)(oba)\}.4H_2O]_a$ $[\{Cd_{1/2}L_{1/2}(nipa)_{1/2}(H_2O)_{1/2}\}$ $(DMF)_{1/2}(H_2O)_a$	DIPA	Turn OFF	6.76 µM 2.39 µM	5
3	Zr-BTDB	MA	Turn ON	0.066 µM	6
4	$[Ln_2(L^2)_2(DMF)_2(H_2O)_4]. H_2O.DMF$ (Ln = Pr; Sm; Eu; Gd; Dy; Ho)	DIPA TEA	Turn OFF	16.4 µM 15.7 µM	7
5	Al MOF	TEA	NA	3 µM	8

Abbreviation: **H_3btc** = benzene tricarboxylic acid; **L** = N^2,N^6-di(pyridin-4-yl)naphthalene-2,6-dicarboxamide; **4, 4′-H_2oba** = 4, 4′-oxybisbenzoic acid; **5-H_2nipa** = 5-nitroisophthalic acid; **BTDB** = 4,4′-(benzo[c][1,2,5]thiadiazole-4,7-diyl) dibenzoic acid; ; **H_3L^2** = 5-(2- nitro-4-carboxylphenyl)isophthalic acid; **Al-MOF** = Aluminium Metal Organic Framework

Section S4: Mixed Matrix Membrane (MMM) studies

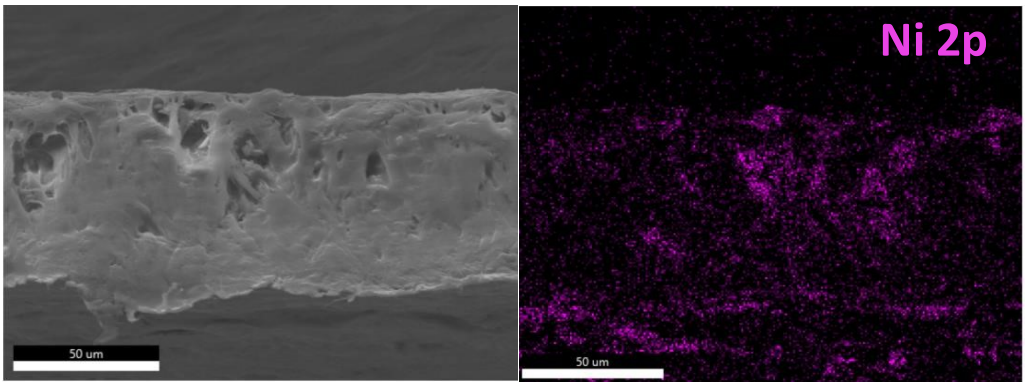

Figure S19. The EDS mapping image of **Ni-*btc* NS MMM** cross section area.

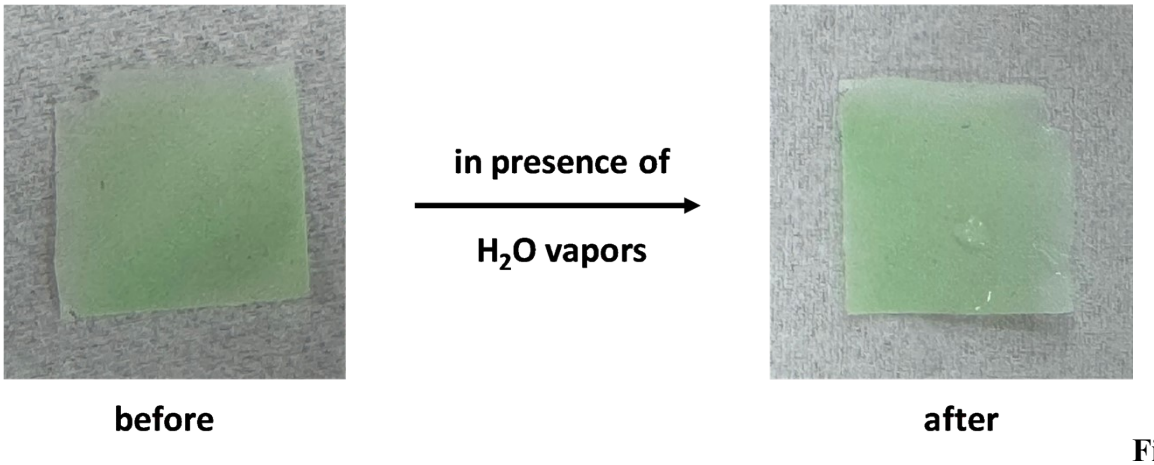

Figure S20. **Ni-*btc* NS MMM** upon exposure to water vapors.

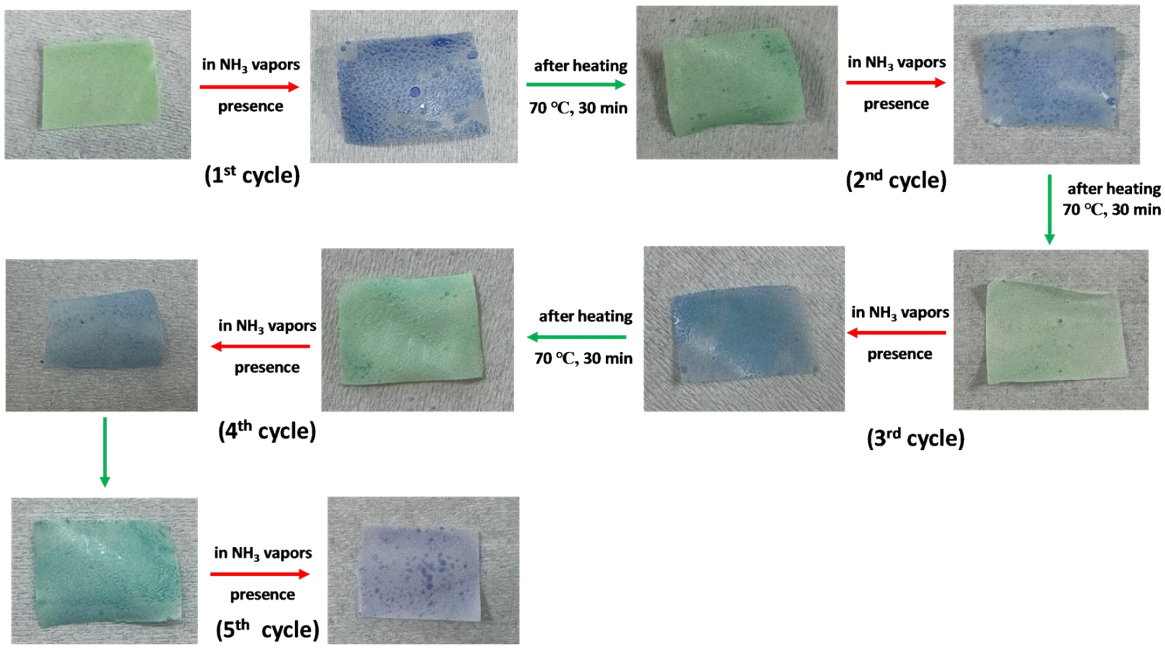

Figure S21. Visible color change of **Ni-*btc* NS MMM** upon exposure to NH_3 vapors for five consecutive cycles.

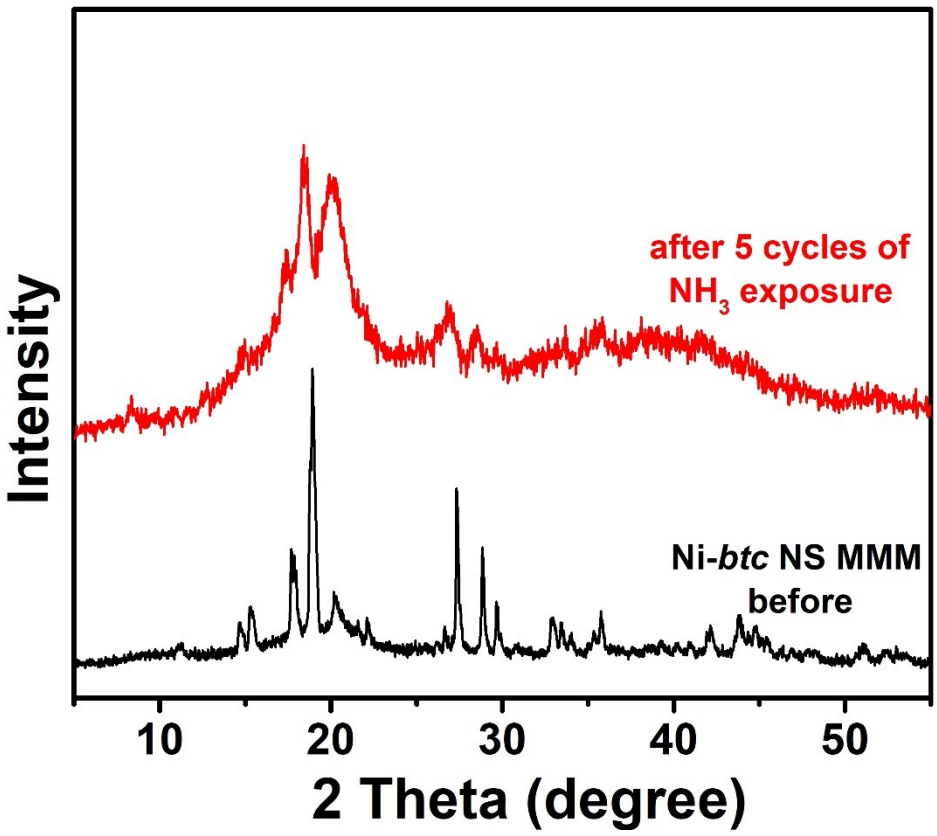

Figure S22. PXRD of **Ni-*btc* NS MMM** after exposure to NH_3 vapors for five consecutive cycles**.**

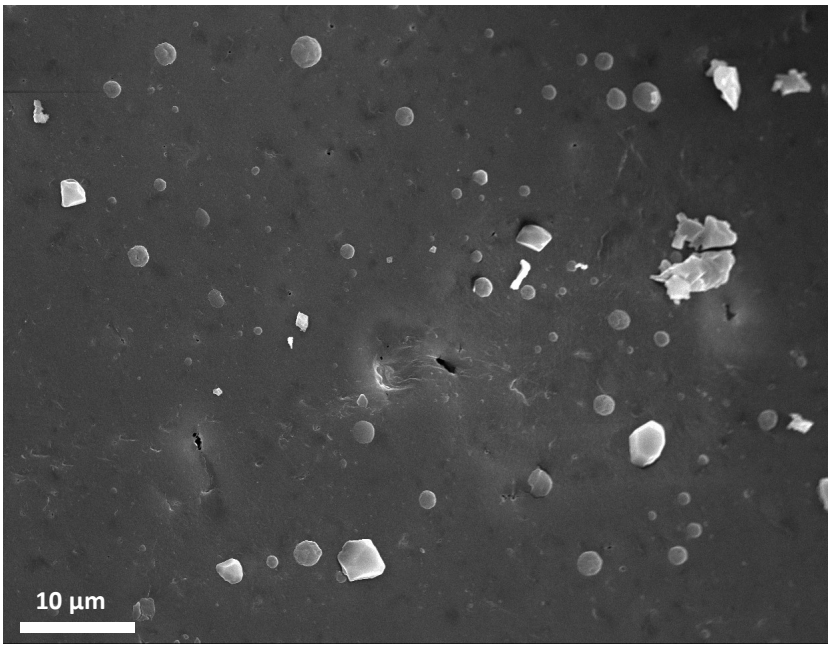

Figure S23. FESEM of Ni-btc NS MMM after exposure to NH_3 vapors for five consecutive cycles.

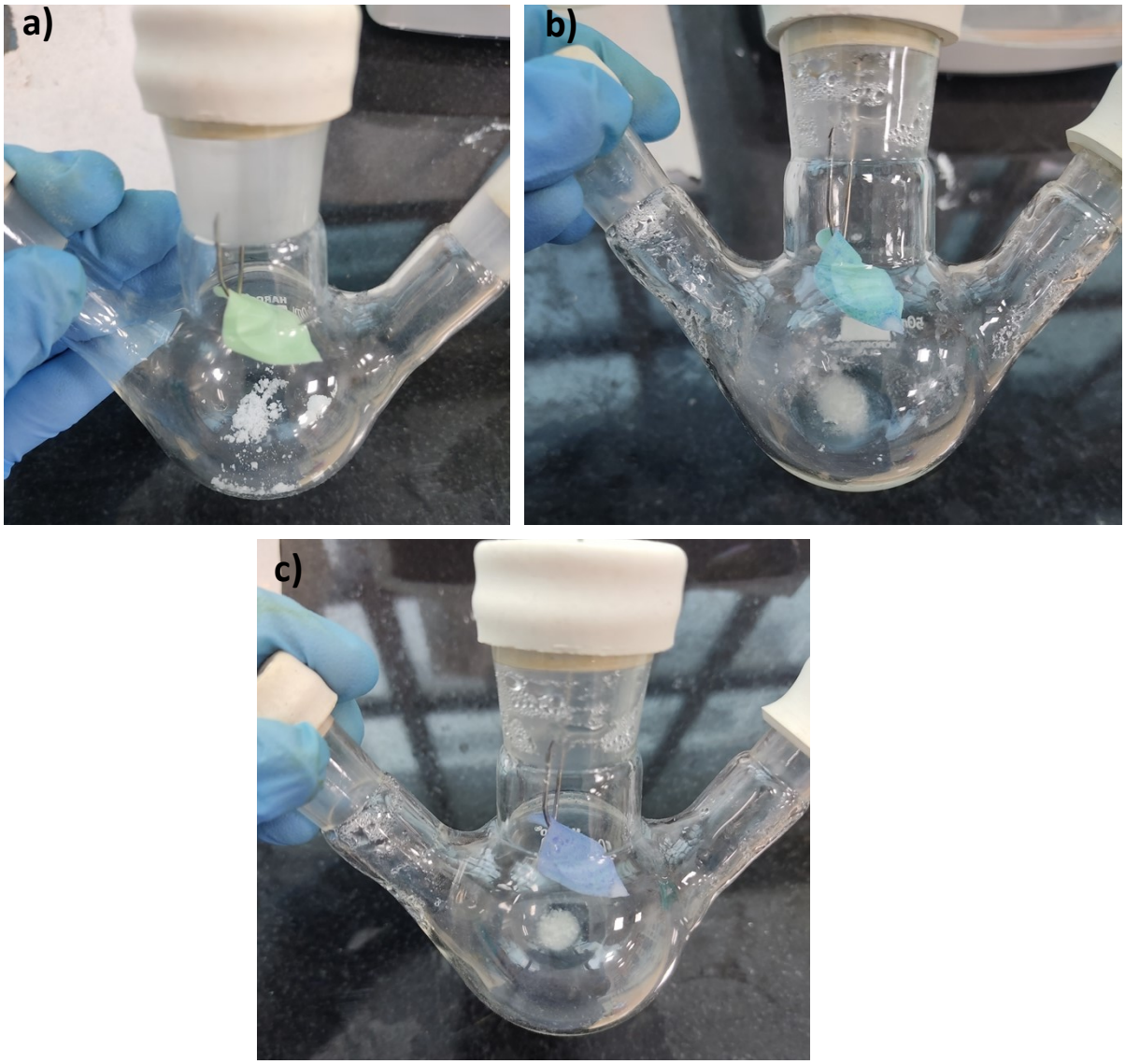

Figure S24. Experimental setup for ammonia sensing from chemical reaction with **Ni-*btc* NS MMM** a) before b) in between and c) after reaction completion

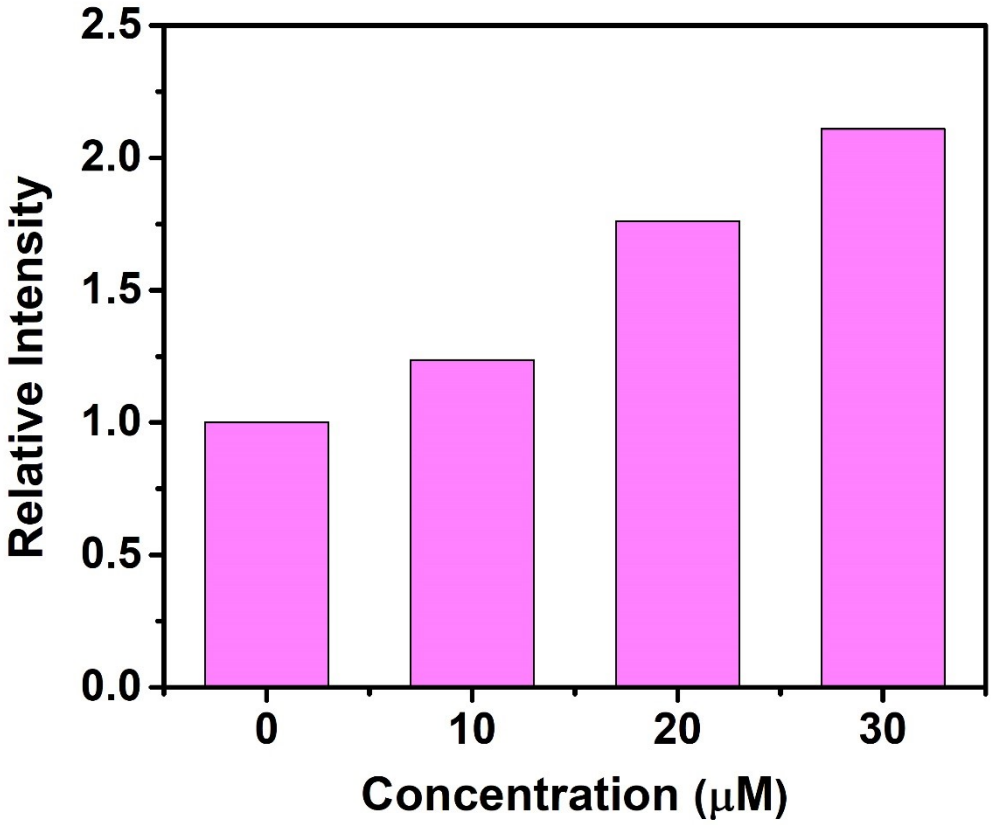

Figure S25. Results of the fluorescence sensing experiment with model contaminated wastewater.

Table S5: Model contaminated wastewater study

Spiked NH_3 (aq.) concentration (μM)	**Found (μM)**	**RC (%)**
10	9.386	93.86
20	19.711	98.55
30	28.758	95.86

- RC %, Recovery percent

References:

1. Frisch, M. J.; Trucks, G. W.; Schlegel, H. B.; Scuseria, G. E.; Robb, M. A.; Cheeseman, J. R.; Scalmani, G.; Barone, V.; Mennucci, B.; Petersson, G. A.; Nakatsuji, H.; Caricato, M.; Li, X.; Hratchian, H. P.; Izmaylov, A. F.; Bloino, J.; Zheng, G.; Sonnenberg, J. L.; Hada, M.; Ehara, M.; Toyota, K.; Fukuda, R.; Hasegawa, J.; Ishida, M.; Nakajima, T.; Honda, Y.; Kitao, O.; Nakai, H.; Vreven, T.; Montgomery, J. A.; Peralta, J. E.; Ogliaro, F.; Bearpark, M.; Heyd, J. J.; Brothers, E.; Kudin, K. N.; Staroverov, V. N.; Kobayashi, R.; Normand, J.; Raghavachari, K.; Rendell, A.; Burant, J. C.; Iyengar, S. S.; Tomasi, J.; Cossi, M.; Rega, N.; Millam, J. M.; Klene, M.; Knox, J. E.; Cross, J. B.; Bakken, V.; Adamo, C.; Jaramillo, J.; Gomperts, R.; Stratmann, R. E.; Yazyev, O.; Austin, A. J.; Cammi, R.; Pomelli, C.; Ochterski, J. W.; Martin, R. L.; Morokuma, K.; Zakrzewski, V. G.; Voth, G. A.; Salvador, P.; Dannenberg, J. J.; Dapprich, S.; Daniels, A. D.; Farkas; Foresman, J. B.; Ortiz, J. V; Cioslowski, J.; Fox, D. J. Gaussian 09, Revision B.01; Gaussian, Inc., Wallingford, CT, 2009.

2. D. I. Pavlov, T. S. Sukhikh, A. A. Ryadun, V. V. Matveevskaya, K. A. Kovalenko, E. Benassi, V. P. Fedin and A. S. Potapov, *J. Mater. Chem. C*, 2022, **10**, 5567–5575.

3. Y. P. Li, S. N. Li, Y. C. Jiang, M. C. Hu and Q. G. Zhai, *Chem. Commun.*, 2018, **54**, 9789–9792.

4. J. Ma, T. Zhou, T. Ma, Z. Yang, J. H. Yang, Q. Guo, W. Liu, Q. Yang, W. Liu and T. Yang, *Cryst. Growth Des.*, 2021, **21**, 383–395.

5. P. Rani, A. Husain, K. K. Bhasin and G. Kumar, *Inorg. Chem.*, 2022, **61**, 6977–6994.

6. A. Mallick, A. M. El-Zohry, O. Shekhah, J. Yin, J. Jia, H. Aggarwal, A. H. Emwas, O. F. Mohammed and M. Eddaoudi, *J. Am. Chem. Soc.*, 2019, **141**, 7245–7249.

7. H. Huang, W. Gao, X. M. Zhang, A.-M. Zhou and J. P. Liu, *CrystEngComm*, 2019, **21**, 694–702.

8. J. Ni, M.-Y. Li, Z. Liu, H. Zhao, J.-J. Zhang, S.-Q. Liu, J. Chen, C.-Y. Duan, L.-Y. Chen and X.-D. Song, *ACS Appl. Mater. Interfaces*, 2020, **12**, 12043–12053.